Roussin's Black Selenium Salt Mössbauer Data

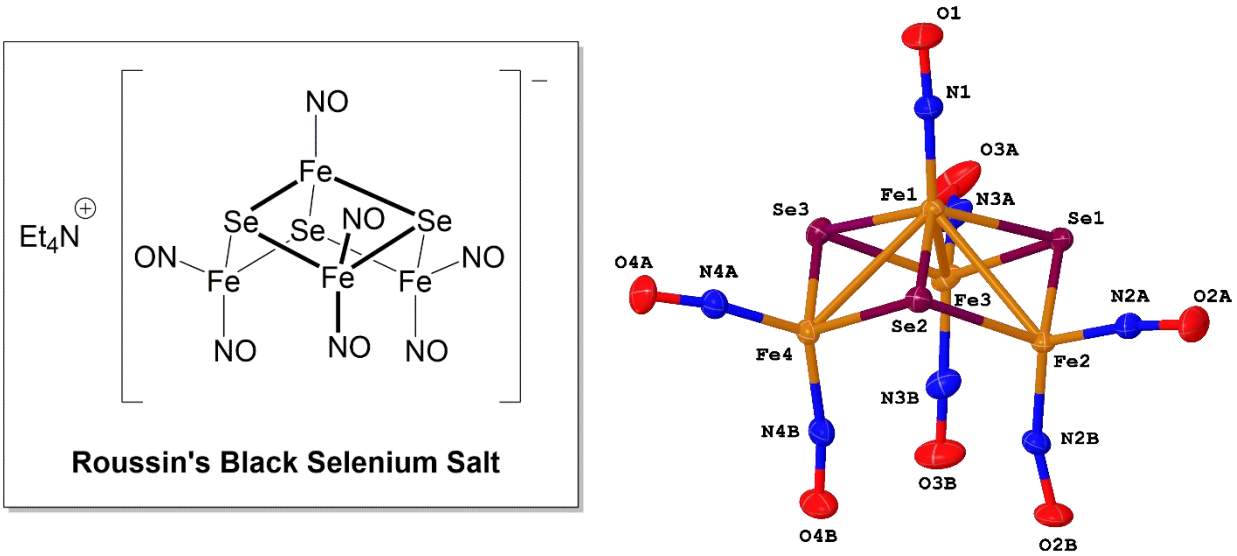

Figure 1. Roussin's Black Selenium Salt (left) and crystal structure (right; tetraethylammonium omitted for clarity).

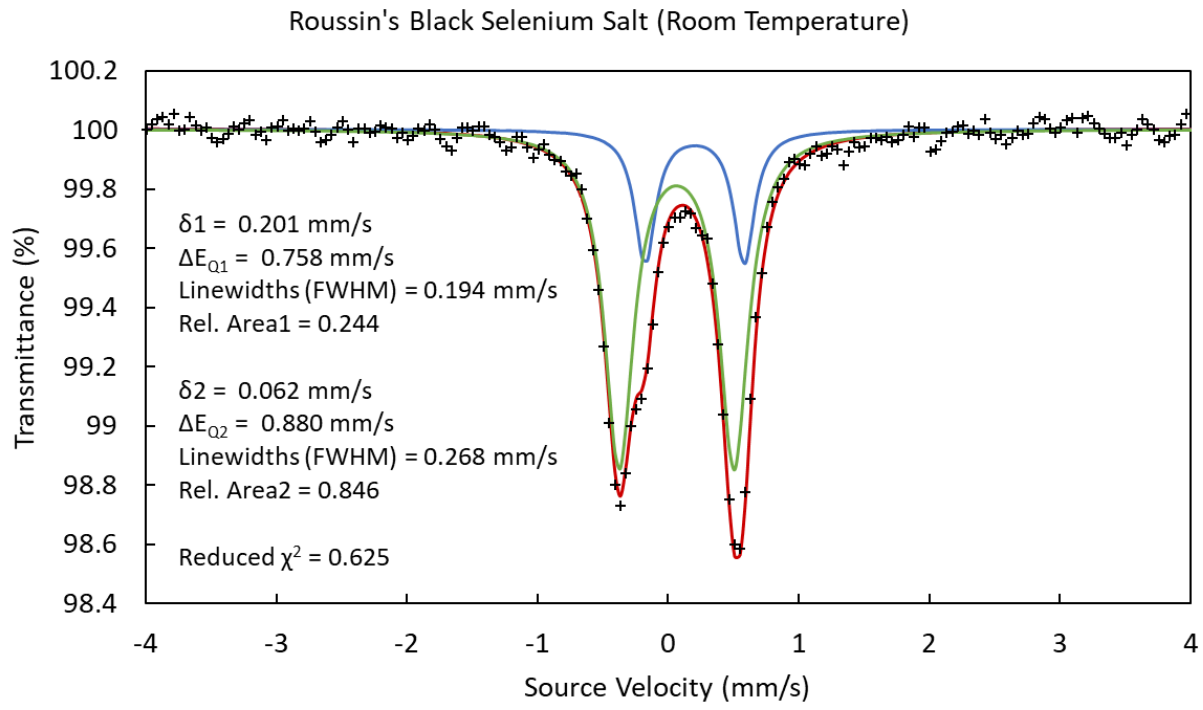

Figure 2. Mössbauer data for Roussin's Black Selenium Salt collected at 294 K. Raw data are depicted with black + signs, the overall fit to the data as the red trace, and the quadrupole doublets fit to the data as the green and blue traces. The parameters δ_1, ΔE_{Q1}, and Rel. Area1 correspond to the minor signal (blue trace) and the parameters δ_2, ΔE_{Q2}, and Rel. Area2 to the major signal (green trace). The reduced χ^2 value of 0.625 for the fit is indicative of a good model of the data.

Roussin's Black Selenium Salt (Figure 1) was synthesized and characterized by single-crystal X-ray diffraction. The corner-vacant cubane structure of the compound contains Fe atoms that reside in two distinct chemical environments. The apical Fe is coordinated by one NO ligand and three bridging Se^{2-} ligands, while the three basal Fe centers are coordinated by two NO ligands and two bridging Se^{2-} ligands. The average Fe_{apical}–Fe_{basal} distance was 2.777(1) Å (from the crystal structure), slightly elongated compared to a typical Fe–Fe single bond (~2.5 Å), but nonetheless indicative of a bond order between 0 and 1 for each Fe_{apical}–Fe_{basal} distance. The near-linearity of the Fe–N–O bond angles (Fe_{apical}–N–O = 177.3(1) °, avg. Fe_{basal}–N–O = 167.8(1) °) suggests that the NO ligands are three-electron donors and should be assigned as NO^+ ligands. Taking into account the overall negative charge of the complex as well as the charges of the Se^{2-} and NO^+ ligands, one could assign two of the Fe oxidation states as Fe(–I) and the other two as Fe(0). However, in order to preserve the C_{3v} symmetry of the compound, it is more satisfactory to assign the three basal Fe centers as Fe(–I) and the apical Fe center as Fe(I).

Mössbauer data (obtained at 294 K) was collected for this compound (Figure 2). Two quadrupole doublets, one for each chemically non-equivalent Fe, were fit to the data to yield the red trace shown in the figure above. The green and blue traces are the two quadrupole doublets; the green trace corresponds to the three basal Fe centers, while the blue trace corresponds to the apical Fe. The relative area of the major signal was 0.846 and the relative area of the minor signal was 0.244. When renormalized such that the total area is unity, this corresponds to 0.776 for the major signal and 0.223 for minor signal, in good agreement with the predicted areas of 0.750 and 0.250 for the major and minor signals respectively. The major signal has an isomer shift of 0.062 mm/s and a quadrupole splitting of 0.880 mm/s. The minor signal has an isomer shift of 0.201 mm/s and a quadrupole splitting of 0.758 mm/s. After running a geometry optimization calculation on the anionic complex, and ensuring the complex was at an energetic minimum by conducting a numerical frequency calculation, isomer shifts were calculated for the complex using the calibration for the B3LYP hybrid functional with a TZVPP basis set developed by Neese.[1] The average calculated isomer shift for the basal irons was 0.050 mm/s and the calculated isomer shift for the apical iron was 0.182 mm/s, in good correlation to the experimental values. The level of computational theory used in the calculations was UKS RIJCOSX-B3LYP-D3 def2-TZVPP def2/J def2-TZVPP/C.[2-8] The isomer shifts and quadrupole splittings for both signals are both consistent with high-spin (S = 5/2 in a tetrahedral ligand field) Fe(III) centers.[9, 10] These oxidation state assignments contradict the assignments given by the simplistic electron counting method employed above and imply that the nitrosyl ligands must be more reduced than initially predicted. Each nitrosyl ligand must therefore be considered as NO^- to account for the overall negative charge of the complex. Considering the NO ligands as NO^- is consistent with the average crystallographic N–O bond distance of 1.178(2) Å, close to a typical N=O bond length.

To assess the overall spin state of the complex, the high-spin Fe(III) centers (S = 5/2) must be considered along with any other ligands that possess unpaired electrons. Each NO^- is S = 1 since each ligand has two unpaired electrons, one in each of the π* orbitals. The closed-shell Se^{2-} ligands are S = 0 and need not be considered. Because the sulfur analogue of this complex (Roussin's Black Salt) is known to be a diamagnetic species (S = 0),[11] it is expected that this compound possesses similar magnetic properties. Thus, the spins of the seven NO^- ligands and the Fe(III) centers must align in such a way as to produce an S = 0 state. The π* orbitals of the NO^- ligands are similar in energy to the d-orbitals of the Fe(III) centers and have the proper symmetry to overlap constructively with some of the Fe(III) d orbitals to lower their energy (necessarily also forming empty orbitals that are more antibonding due to destructive overlaps). It is therefore necessary to count the electrons of the Fe(III) d orbitals with the electrons in the π^* orbitals of the NO ligands. Employing the Enemark-Feltham notation[12] for electron counting, the apical unit should be treated as $\{FeNO\}^7$, while the three basal units should be treated as $\{Fe(NO)_2\}^9$. This means that there should be three unpaired electrons (S = 3/2) on the $\{FeNO\}^7$ unit, and one unpaired electron (S = 1/2) on each of the basal $\{Fe(NO)_2\}^7$ units. Aligning the three S = 1/2 $\{Fe(NO)_2\}^9$ units antiparallel to the apical S = 3/2 $\{FeNO\}^7$ unit gives the correct S = 0 spin state for the complex overall.

Thus, the basal $\{Fe(NO)_2\}$ units are antiferromagnetically coupled to the apical $\{FeNO\}^7$ unit. Given that this method of electron counting is consistent with the experimental Mössbauer data, the probable spin state of the complex, the overall negative charge of the complex, and the crystallographically measured average bond distances within the complex, the resulting bonding model is adequate. The final bonding model is depicted in Figure 3 below.

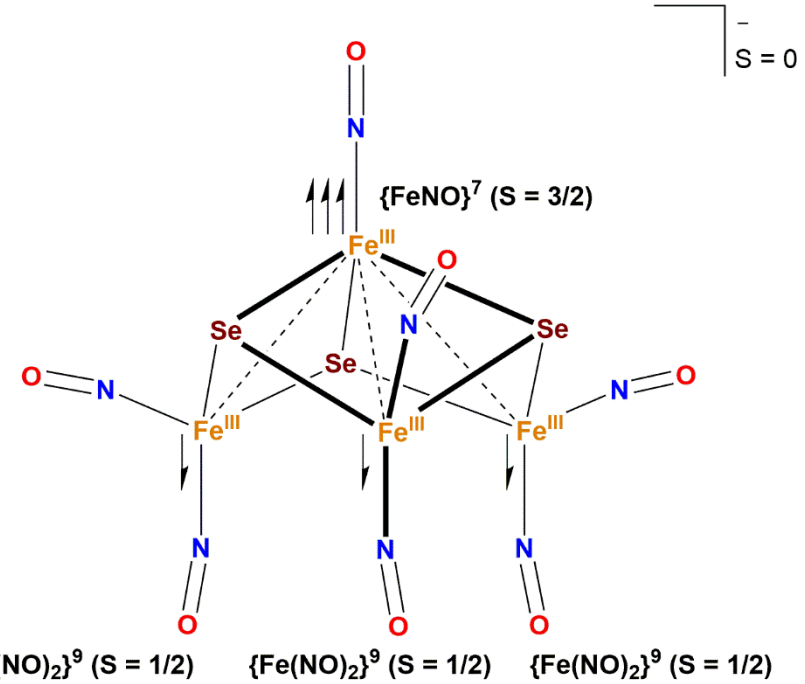

Figure 3. Bonding model for Roussin's Black Selenium Salt accounting for all experimental data. The dashed lines between the Fe(III) centers indicate a bond with a bond order in between 0 and 1. The three S = 1/2 $\{Fe(NO)_2\}^9$ basal units are antiferromagnetically coupled to the apical S = 3/2 $\{FeNO\}^7$ unit, giving the correct S = 0 spin state for the complex. Each Fe center is high-spin Fe(III) while each NO ligand is treated as NO^- to account for the overall 1– charge. This bonding model is identical to the bonding model for the analogous sulfur compound, Roussin's Black Salt.[13, 14]

Mössbauer data were collected with a See Co model W304 resonant gamma-ray 1024 channel spectrometer with a ^{57}Co on Rh foil source. The velocity range used for data collection was ± 10 mm/s. The data collection was conducted with the sample under vacuum. Mössbauer data were fit using the WMOSS4F software package. The theoretical model used to fit the Mössbauer data was to fit two quadrupole doublets to the experimental data, each doublet corresponding to one type of Fe signal. The fitting method used for each fit was an adaptive nonlinear least-squares algorithm developed by Dennis et al. in 1981 available within the WMOSS4F software.[15] The parameters fit for each quadrupole doublet were their isomer shifts (δ), quadrupole splittings (ΔEQ), linewidths (the FWHM), and their relative areas (i.e. their peak integrations).

Information on the crystallographic data is included below.

Crystal Data

$(C_8H_{20}N)[Fe_4N_7O_7Se_3]$	Z = 8
M_r = 800.590	Mo $K\alpha$ radiation (λ = 0.71073 Å)
Monoclinic, $C2/c$	μ = 7.064 mm^{-1}
a = 20.73(1) Å	T = 100 K
b = 12.77(1) Å	Block, black

c = 18.50(2) Å
β = 104.96(1)°
V = 4732(1) Å^3

0.35 x 0.15 x 0.078 mm

Data Collection

Bruker APEX-II CCD
area-detector
diffractometer
Absorption correction:
multi-scan
(SADABS-2016/2[5])
T_{min} = 0.271, T_{max} = 0.714

62840 measured reflections
61456 independent reflections
5898 reflections with $F_0 > 4\sigma(F_0)$
R_{int} = 0.0266

Refinement

$R[F_0 > 4\sigma(F_0)]$ = 0.0150
$wR2$ = 0.0355
GooF = 1.0640
6375 reflections

333 parameters
H-atom parameters constrained
$\Delta\rho_{max}$ = 0.42 e Å^{-3}
$\Delta\rho_{min}$ = -0.35 e Å^{-3}

Table 1

Selected geometric parameters (Å, °)

Se1–Fe1	2.332(1)	Fe2–N2A	1.670(2)
Se1–Fe2	2.378(2)	Fe2–N2B	1.680(1)
Se1–Fe3	2.382(2)	Fe3–N3A	1.676(2)
Se2–Fe1	2.339(2)	Fe3–N3B	1.677(2)
Se2–Fe2	2.381(1)	Fe4–N4A	1.676(2)
Se2–Fe4	2.378(2)	Fe4–N4B	1.678(2)
Se3–Fe1	2.334(2)	O1–N1	1.177(2)
Se3–Fe3	2.374(1)	O2A–N2A	1.175(2)
Se3–Fe4	2.374(2)	O2B–N2B	1.179(2)
Fe1–Fe2	2.787(1)	O3A–N3A	1.180(2)
Fe1–Fe3	2.783(1)	O3B–N3B	1.178(2)
Fe1–Fe4	2.761(2)	O4A–N4A	1.180(2)
Fe1–N1	1.666(1)	O4B–N4B	1.174(2)
Fe2–Se1–Fe3	101.195(9)	O1–N1–Fe1	177.3(1)
Fe4–Se2–Fe2	102.11(2)	O2A–N2A–Fe2	170.8(1)
Fe3–Se3–Fe4	101.86(2)	O2B–N2B–Fe2	160.1(1)
Se1–Fe1–Se2	108.76(2)	O3A–N3A–Fe3	169.4(2)
Se1–Fe1–Se3	108.81(2)	O3B–N3B–Fe3	167.1(1)
Se3–Fe1–Fe2	109.496(9)	O4A–N4A–Fe4	169.5(1)
		O4B–N4B–Fe4	169.9(1)

Data collection: *SMART*[16]; cell refinement: *SAINT*[16]; data reduction: *SAINT*; program(s) used to solve structure: *SHELXTL*[17]; program(s) used to refine structure: *SHELXL*[18]; molecular graphics: *OLEX2*[19]; software used to prepare material for publication: *OLEX2*.

References:

1. Römelt, M.; Ye, S.; Neese, F. *Inorg. Chem.* **2009**, *48*, 784–785.
2. Neese, F. *WIREs Comput. Mol. Sci.* **2012**, *2*, 73–78.
3. Neese, F. *WIREs Comput. Mol. Sci.* **2018**, 8:e1327.
4. Grimme, S.; Ehrlich, S.; Goerigk, L. *J. Comput. Chem.* **2011**, *32*, 1456–1465.
5. Grimme, S.; Antony, J.; Ehrlich, S.; Krieg, H. *J. Chem. Phys.* **2010**, *132*, 154104.
6. Weigend, F.; Ahlrichs, R. *Phys. Chem. Chem. Phys.* **2005**, *7*, 3297–3305.
7. Weigend, F. *Phys. Chem. Chem. Phys.* **2006**, *8*, 1057–1065.
8. Hellweg, A.; Hattig, C.; Hofener, S.; Klopper, W. *Theor. Chem. Acc.* **2007**, *117*, 587–597.
9. Greenwood, N. N.; Gibb, T. C. Mössbauer Spectroscopy; Chapman and Hall Ltd: London, 1971; pp 91.
10. Gütlich, P.; Bill, E.; Trautwein, A. X. Mössbauer Spectroscopy and Transition Metal Chemistry: Fundamentals and Applications; Springer-Verlag Berlin Heidelberg, 2011; pp 85.
11. Cambi, L.; Szegö, L. *Rendiconti Lincei* **1931**, *12*, 168–172.
12. Enemark, J. H.; Feltham, R. D. *Coord. Chem. Rev.* **1974**, *13*, 339–406.
13. Jaworska, M.; Stasicka, Z. *J. Mol. Struct.* **2006**, *785*, 68–75.
14. Hopmann, K. H.; Noodleman, L.; Ghosh, A. *Chem. Eur. J.* **2010**, *16*, 10397–10408.
15. Dennis, J. E.; Gay, D. M.; Walsh, R. E. *ACM Trans. Math. Softw.* **1981**, *7*, 348–368.
16. Bruker-AXS (2016). *SADABS*, *SMART*, and *SAINT*. Bruker AXS Inc., & APEX3. Version 2016.5-0. Madison, Wisconsin, USA.
17. Sheldrick, G.M. *Acta Cryst.* **2008**, *A64*, 112–122.
18. Sheldrick, G.M. *Acta Cryst.* **2015**, *C71*, 3–8.
19. Dolomanov, O. V.; Bourhis, L. J.; Gildea, R. J.; Howard, J. A. K.; Puschmann, H. *J. Appl. Cryst.* **2009**, *42*, 339–341.